EUROPEAN ORGANIZATION FOR NUCLEAR RESEARCH

CERN-INTC-2004-006

INTC-P-86 Add. 2

22 January, 2004

Studies of High-T_C Superconductors Doped with Radioactive Isotopes

REQUEST OF ADDITIONAL BEAM TIME TO IS360 - ADDENDUM 2 -

(*) Aveiro[1], Grenoble[2], Leipzig[3], Lisboa[4], Porto[5], Sacavém[6] and the ISOLDE/CERN Collaboration[7]

E. Alves[6], J.C. Amaral[1], V.S. Amaral[1], J.P. Araújo[5], P. Bordet[2], J.G. Correia[4,6,7], S. Dias[4], A. L. Lopes[1], A. C. Marques[4], T. M. Mendonça[5], H. Haas[6], Ph. Odier[2], M.S. Reis[1], E. Rita[4,6], J.C. Soares[4], J.B. Sousa[5], W. Tröger[3]

Spokesperson and contact person: J.G. Correia

ABSTRACT

The IS360 collaboration proposes to study the atomic ordering of oxygen, O_δ, and fluorine, F_δ, atoms which go to the Hg planes of the $HgBa_2Ca_{n-1}Cu_nO_{2n+2+\delta}$, family of high-Tc superconductors.

Being weakly bound within the structure, O_δ and F_δ, have similar chemistry and ionic radius and act as non-stoichiometric dopants. While the injection of holes at the Cu planes is known to depend on δ, being proportional to their nominal ionic charges -2 and -1, the ionic efficiency of the doping has been experimentally questioned, mainly because the local structure of the Hg planes containing the O or F dopants was not firmly established.

At ISOLDE ^{199m}Hg radioactive nuclei are implanted to low doses. After annealing under controlled atmosphere, the perturbed angular correlation technique, PAC, measures the electric field gradients, EFGs, which contain information about the local neighboring of Hg. With PAC we have shown that both O_δ and F_δ, occupy the center of the Hg mesh and implicitly shown that interstitial F_δ, aligns along [100] and [010] directions when in high concentrations in $HgBa_2CuO_{4+\delta}$ (n=1, Hg1201).

Since such atomic effect of the dopant can contribute to define separate charge regions, we intend to study $HgBa_2Ca_2Cu3O_{8+\delta}$ (n=3, Hg1223), which has the highest Tc ever registered at ambient pressure of 135K for δ(oxygen) ~ 0.46. These experiments are viable, particularly due to the natural high concentration of O_δ for n > 1 on single-phase powder samples. Epitaxial thin films will be used to provide the measurement of the orientation of the EFGs on the lattice. To interpret the data, self consistent first principle calculations of the charge distribution including lattice relaxation are performed. The EFG is then calculated at the Hg sites as a function of different O_δ and F_δ concentrations and configurations.

* Institute addresses are shown on page 2.

Institute addresses:

1 Physics Dept., Univ. Aveiro, P-3800 Aveiro, Portugal

2 Lab. de Cristallographie, CNRS, Av. des Martyrs 25, F-38042 Grenoble CEDEX 9, France

3 Fak. für Physik und Geowissenschaften, Univ. Leipzig, Linnéstraβe 5, D-04103 Leipzig, Germany

4 CFNUL, Av. Prof. Gama Pinto 2, P-1699 Lisboa Codex, Portugal

5 IFIMUP, Fac. Ciências, Rua do Campo Alegre 657, P-4150 Porto, Portugal

6 Instituto Tecnológico e Nuclear, E.N. 10, P-2685 Sacavém, Portugal

7 HP Div., CERN, CH-1211 Geneva 23, Switzerland.

INDEX **page**

1 Foreword

17 years after its discovery, high temperature superconductivity still remains one of the most interesting and controversial phenomena in solid state physics [1, 2, 3]. While believing that high temperature superconductivity will lead one day to a technological and economical revolution, today's reality and expectations are more pragmatic due to the difficulty of stabilizing and integrating such complex materials [4]. Scientific research and application "breakthroughs" of the high-Tc superconductors -HTcS- got specialized over the years to few laboratories and industries. Nevertheless, YBaCuO, or more intensively applied compounds like BiSrCaCuO that naturally form pinning centers for fluxons, are used in thin film technologies for microelectronic devices as well as in high current superconducting cables for magnetic coils of electricity transport [5].

So far, the materials where the highest Tcs have been measured and confirmed are of main use and interest in fundamental research. These are described as the $HgBa_2Ca_{n-1}Cu_nO_{2n+2+\delta}$ family of HTcS, which doping mechanisms are addressed in this addendum.

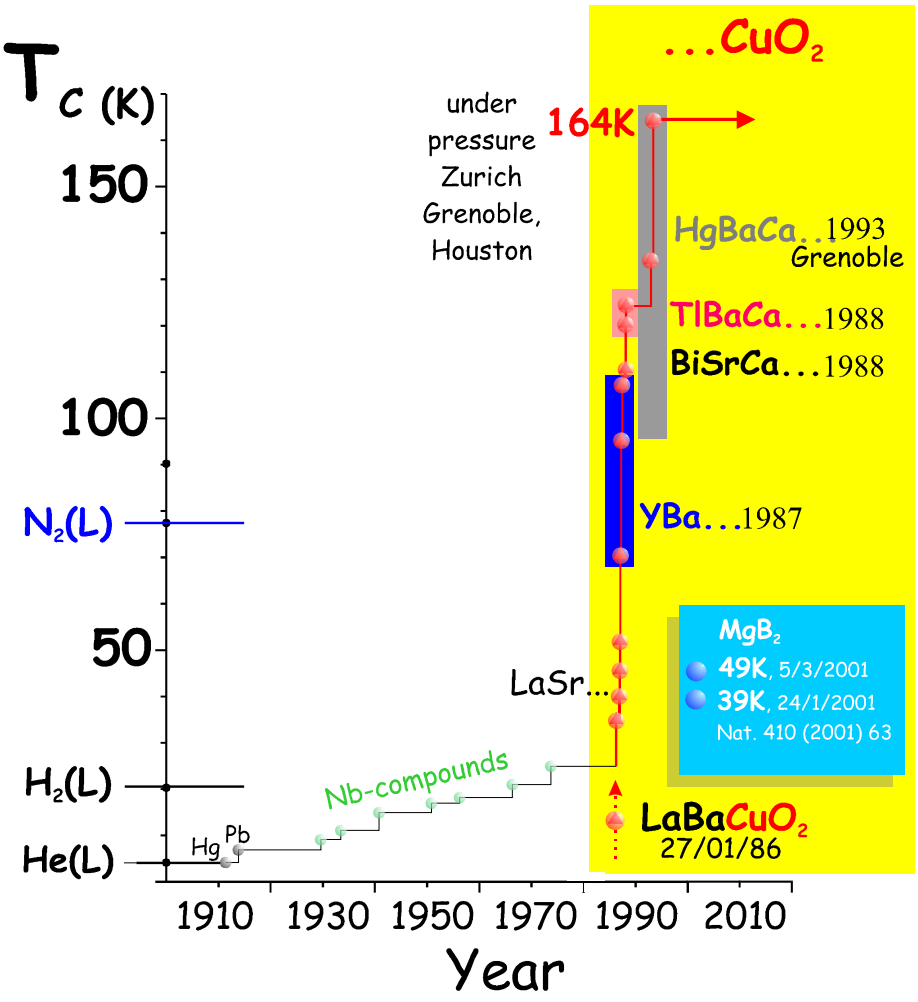

Figure 1 Materials and Tc evolution plot as a function of the discovery year.

2 Status "of the art" in the $HgBa_2Ca_{n-1}Cu_nO_{2n+2+\delta}$ family of HTcS

2.1 Problematic

The compound with the highest critical temperature ever attained (Tc ~ 137K at ambient pressure and 153 K at high-pressure) is the n=3 member of the $HgBa_2Ca_{n-1}Cu_nO_{2n+2+\delta}$, series, with optimum doping δ~0.4 [6]. The simple tetragonal structures of these compounds (Figure 2) motivated intense work to study Tc as a function of the structural parameters variations. Lattice constants and crystallographic parameters, in particular at the Cu planes, have been reported to depend on temperature and concentration of the non-stoichiometric dopant elements at the Hg layers, referred to as the charge reservoirs block [7]. In the past few years the research has concentrated over comparative studies of F^-_δ and O^{2-}_δ doping efficiency. Oxygen and fluorine have similar chemical affinity and ionic radius but differ by one electronic charge. While it has been proven that the injection of holes at the Cu planes is proportional to their nominal ionic charges -2 and -1, the idea that the doping efficiency is simply given by the dopant concentration and ionic charge has been experimentally and theoretical questioned [8].

Structural defects like Hg vacancies, Cu ions (†) or CO_3^{2-} (‡) impurities replacing Hg are often discussed to play a role in the generation of charge carriers at the Cu planes. More simply, in highly pure materials the non-stoichiometric O_δ "alone" might induce local distortions, which could

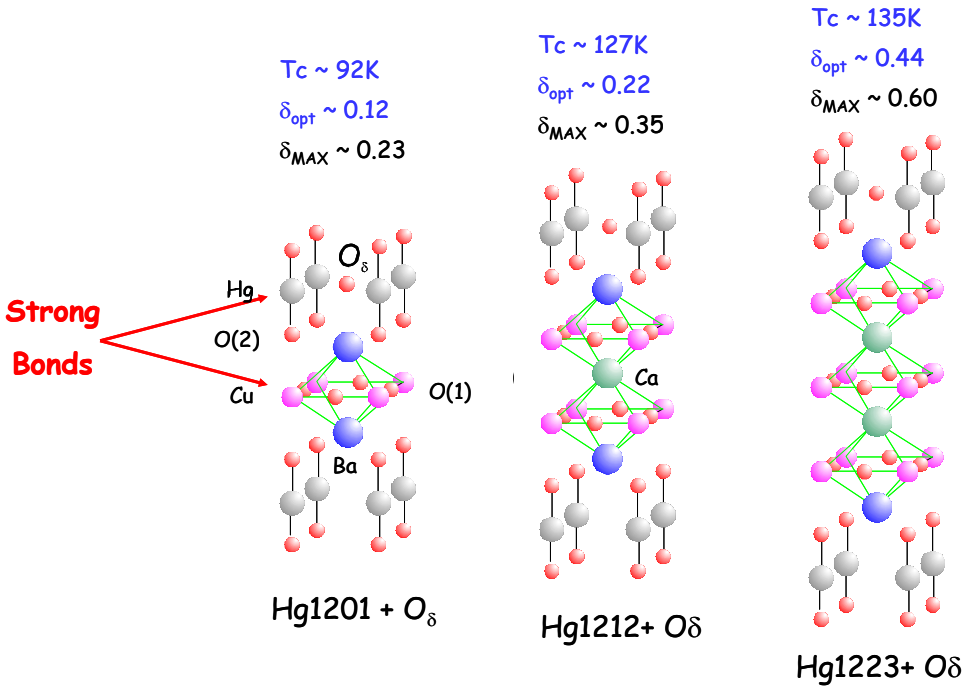

Figure 2 Schematic pictures of the basic elements on the cells of $HgBa_2Ca_{n-1}CunO_{2n+2+\delta}$, for n=1, Hg1201, for n=2, Hg1212 and for n=3, Hg1223. The δ_{oxygen} for optimum doping at highest Tc (δ_{opt}) and maximum δ_{oxygen} (δ_{max}) experimentally measured are also quoted. The two strongest bonds of the structure are stressed: (a) The O(2)-Hg-O(2) dumbbell with the main contributing bonds to the measured EFGs at Hg and the $CuO(1)_2$ bonds that keep the structure well tight. The known charge dopants act at the Hg planes, with Ba and Ca acting as ion charge transfer routes.

(†) Cu replacing Hg as been proposed – and denied! - to exist due to the analogy of Hg1212 with $YBa_2Cu_3O_{6+\delta}$ where Cu occupies the Hg-equivalent places at the charge block reservoir.

(‡) CO_3^{2-} contaminant ions come from undesired carbonates formed with the reacting agents when the compounds are made by high-pressure synthesis.

be of great importance for the doping mechanism [9, 10]. In order to understand these effects x-ray and neutron diffraction studies as well as the local technique EXAFS [11] were used on powder and single crystal samples in Hg1201 [12]. Both methods have shown the existence of local distortions at the Cu planes near Tc, but it was not possible to relate them to the superconductivity mechanism or to the dopant chemical effects.

The findings of spin and charge inhomogeneity in CuO bonds [13] and CuO_2 [14] layers in $YBa_2Cu_3O_{6+\delta}$ stresses the existence of local and non-linear charge ordering in the cuprates. It seems that static charge order is compatible with superconductivity as long as spin order remains dynamic. Such phenomena are currently thought to be due to the segregation of holes away from regions of local antiferromagnetically ordered moments. They lead to the formation of "stripes", i.e. alternating regions at the nanometer scale with different structural and electronic properties. So far it is not known under which conditions such phenomena occur within the materials or whether they are intrinsically related with high-Tc superconductivity, either inhibiting or enhancing it, being this a subject of intense investigation [15].

2.2 IS360 contribution from add. 1

During 2002 we have performed PAC experiments on special powder-like Hg1201 (n=1) samples, consisting of *reduced* material with low oxygen content assigned to be $[O_\delta] < 6\%$. The *principal* component of the EFG, Vzz, and the asymmetry parameter, η, measured at ^{199m}Hg atoms, are the source of information for determining the O_δ and F_δ lattice sites and grouping into the Hg-planes. After implantation of ^{199m}Hg the first step on each sample is to anneal under Ar flow to 190^0C during 18 min. This treatment anneals the implanted region and further avoids/extracts the non-stoichiometric O_δ. The observed EFG is then mainly due to Hg atoms in the O(2)-Hg-O(2) configuration without other specific defects nearby. After the first annealing under Ar, the samples were measured in the presence of oxygen, introduced under pressure, or in the presence of Fluorine introduced via *soft-chemistry* of XeF_2 mixing [8].

Fig 3a shows the typical PAC spectrum obtained in reduced, *R*, samples after Ar annealing, compared with one obtained from our previous work in non reduced Hg1201 [16]. While the EFG parameters are exactly the same, the spectra taken on the reduced samples are of smaller amplitude and look more attenuated as a function of time. The reduction in amplitude is mainly due to an angular anisotropy integration effect since the detectors are now running very close to the sample by almost a factor of 8, due to much smaller and less active samples. The larger attenuation with time, is typical of highly reduced materials and might be due to higher Hg deficiency which can create such EFG distributions. The results for oxygen doping, shown in Figure 3b, have reproduced our previous work [16, 17] showing that O_δ occupies only the center of the Hg planes, this time achieving, due the pressure applied, a higher concentration $\delta_O = 18(2)\%$ in the probed zone.

On the other hand, the results for the fluorine doping are quite impressive, completely changing the fields as a function of the presence of fluorine.

Figure 4a) shows the PAC spectra taken after and during annealing under XeF_2. A main new EFG_3 with lower $\omega_{03} = 890$ Mrad/s and asymmetry parameter $\eta_3 \sim 0.044(4)$ was found. Figure 4b) shows the PAC results measured at room temperature after one last annealing step under Ar, after annealing the samples under XeF_2. Now, a main EFG_4 with parameters $\omega_{04} = 1091(5)$ Mrad/s and asymmetry parameter $\eta_4 \sim 0.22(1)$ was found.

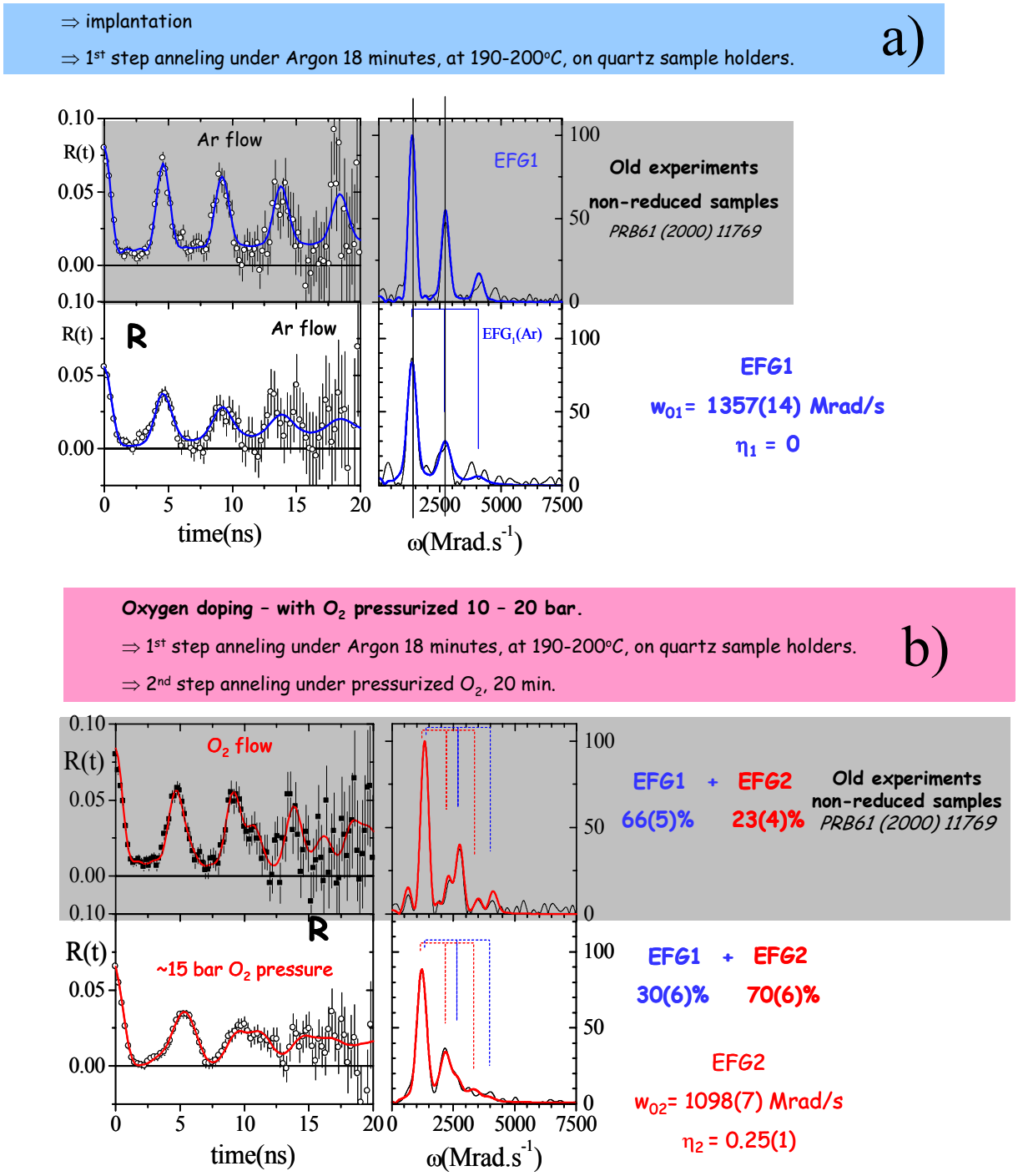

Figure 3 Comparison of R(t) PAC spectra of older experiments performed on non-reduced samples with the data obtained in the present experiments performed on reduced material. a) under Ar anneling. b) under oxygen flow (old samples) and under 15 bar oxygen pressure. The data shows the reproducibility of the EFG parameters, in particular for the ones obtained under oxygen pressure, where the lower frequency and non-zero asymmetry parameter reveal the presence of single O_δ atoms at the center of the Hg mesh [16].

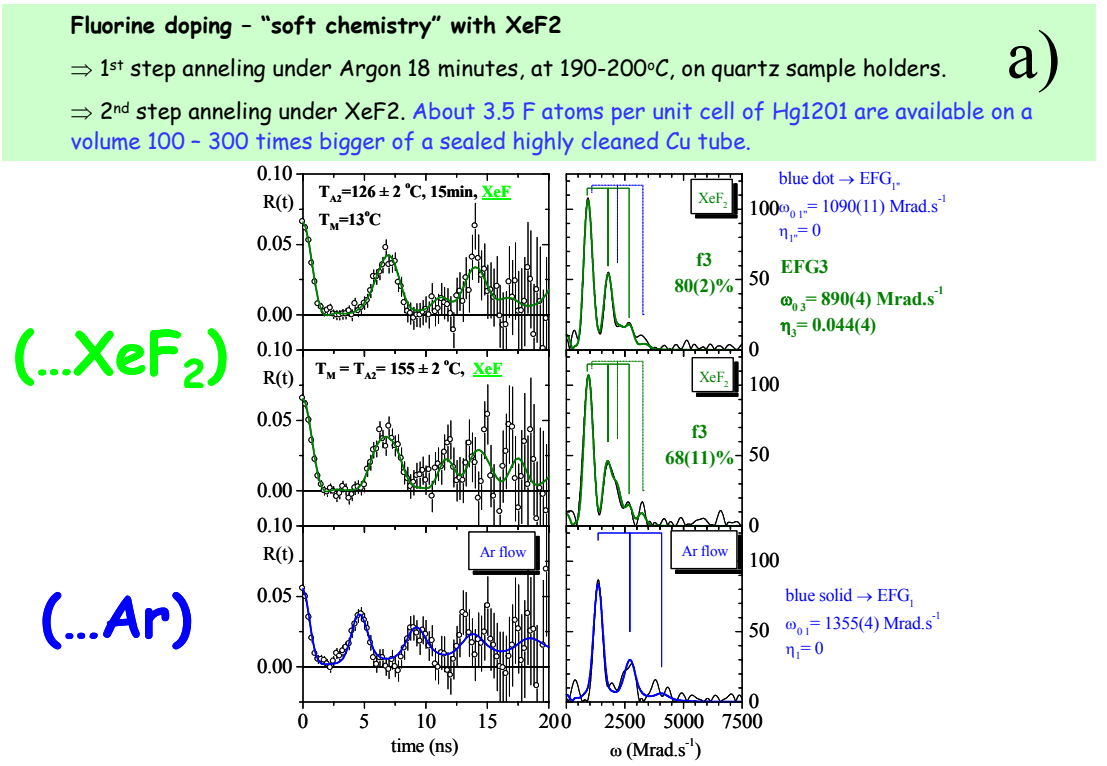

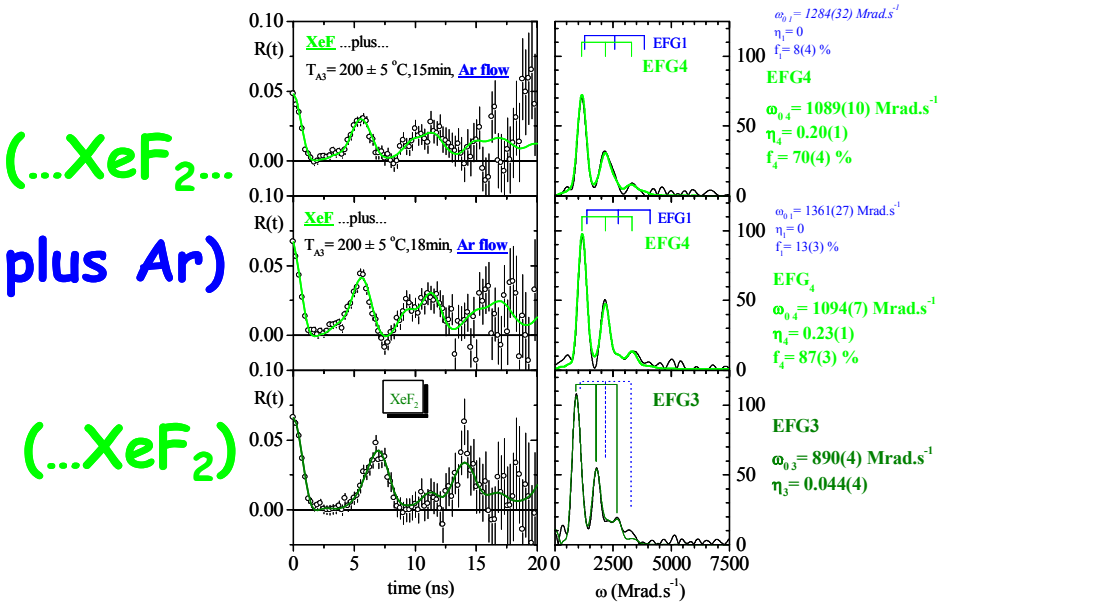

Figure 4 a) PAC spectra taken after and during annealing under XeF2. A main EFG_3 characterized by a low ω_{03} = 890 Mrad/s and asymmetry parameter $\eta_3 \sim 0.044(4)$ was found. The bottom spectrum is the reference result for one step annealing under Ar, here shown for comparison.
b) PAC results measured at RT, after annealing under Ar samples which were previously annealed under XeF_2. The aim is to try extracting fluorine that was previously introduced. A main EFG4 with parameters ω_{04} = 1091(5) Mrad/s and asymmetry parameter $\eta_4 \sim 0.22(1)$ was found. The bottom spectrum was obtained under annealing with only XeF2, here included for comparison.

The data were interpreted with the help of simulated EFGs obtained for different fluorine configurations around Hg atoms. The method is the *full-potential-linearized-augmented-plane-wave (FLAPW) Electronic Structure Method Local-density-approximation (LDA)*, which was already used in our previous work, as well as by other authors on simpler approaches [see references in 16 and 8]. This method generates the charge density within the atomic structure, used afterwards to calculate the EFGs at the Hg site. During 2003 a step forward has been made to improve simulations by implementing methods which allow the relaxation of internal parameters. This is illustrated in Figure 5, where only configurations which produce results compatible with the experimental PAC data are shown.

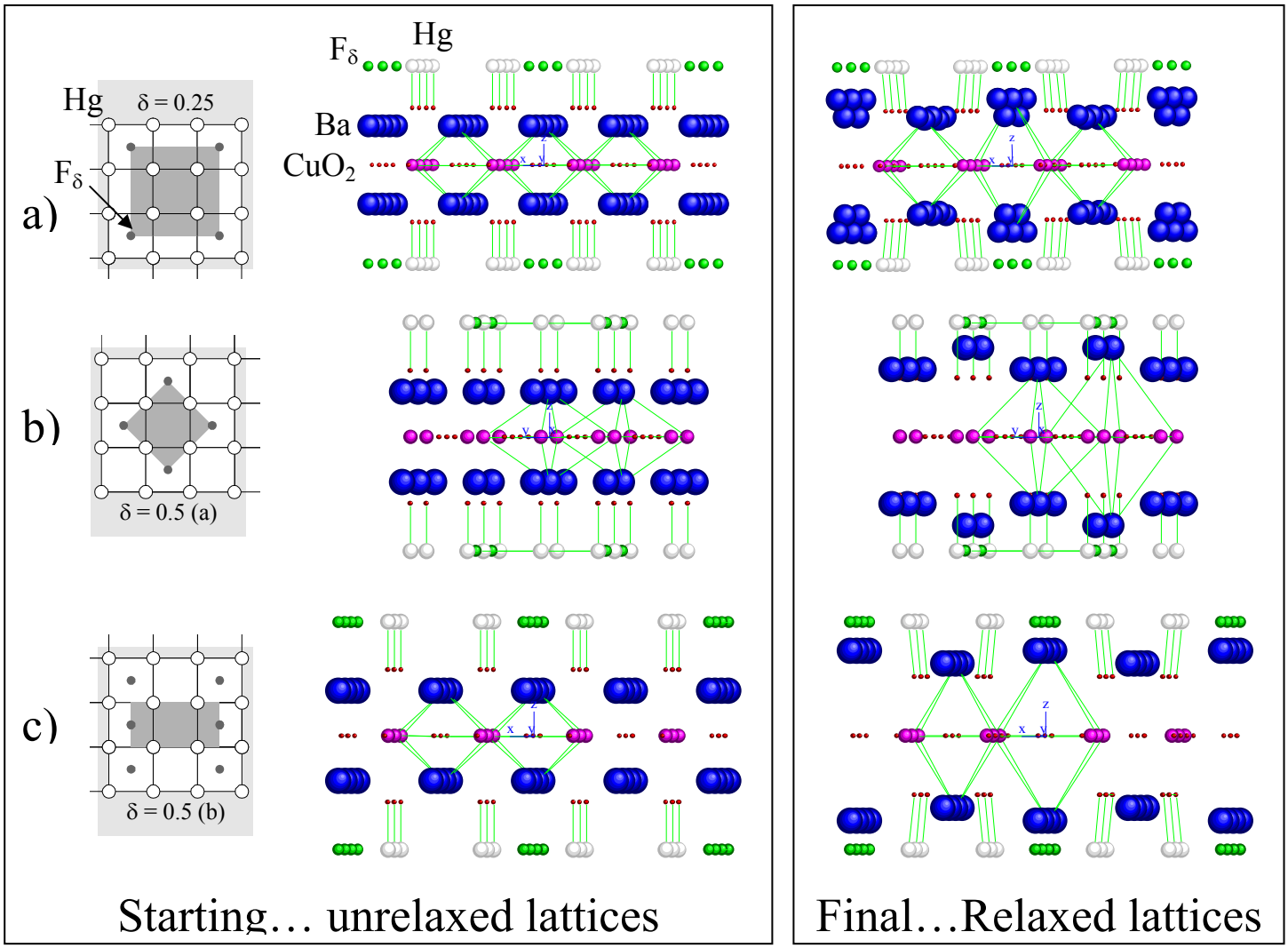

Figure 5 Relaxation effects of the internal parameters of the super cells used to simulate the EFGs for different fluorine configurations at the Hg planes. The figures on the left block represent the starting lattice with initial internal parameters from neutron diffraction data of typical reduced (low Oδ content) samples – these represent ideal non-deformed lattices. The pictures on the right block are generated after relaxation, where the shifts have been amplified by a factor of 10 to become visible. The most striking features are the elongation of O-Hg-O with δF and the Ba strong shifts towards F. A deformation of the Cu planes was also observed but it can hardly be seen in these perspectives.

a) Hg atoms "see" only one F at the center of the Hg square, δF = 0.25;

b) each Hg atom "sees" two F atoms along [110] or [1-10];

c) each Hg atom "sees" two F with a 90° angle, for δF = 0.5. Together, these interstitial F atoms align along [100] or [010].

Figure 6 shows refined neutron diffraction data (dots) of internal parameters of Hg1201 as a function of oxygen and fluorine doping [8 and references therein]. These are compared with the data obtained from relaxation FLAPW simulations for the F doping (dots connected by lines). Relaxation calculations for oxygen doping are in progress.

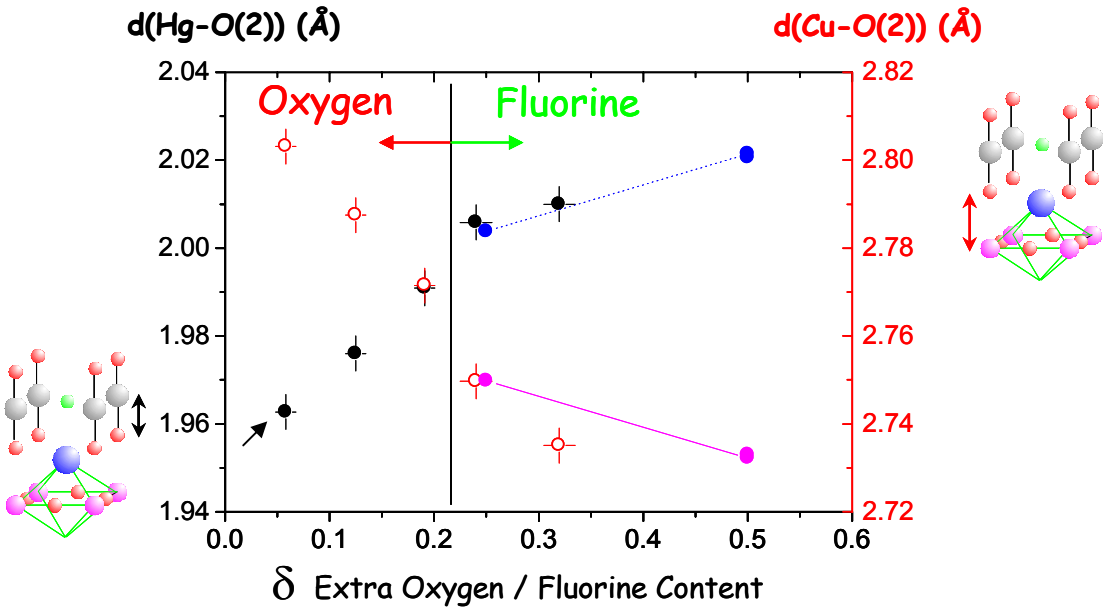

Figure 6 Hg1201 refined neutron diffraction data of d(Hg-O(2)) –closed dots, left axis- and d(Cu-O(2))- open dots, right axis- as a function of oxygen and fluorine doping. In Hg1201 δO is smaller than 0.20, while there are no values reported for δF smaller than 0.24. These are compared with the data obtained from relaxation FLAPW simulations for the F doping (dots connected by lines). Relaxation calculations for oxygen doping are in progress, which need much larger super cells for diluted concentrations.

In figure 7 we resume the experimental |Vzz | and η parameters of the EFGs obtained from different annealing conditions under XeF_2 and Ar, compared with the EFGs obtained from the FLAPW simulations at the Hg site, for the different F configurations. The relevant features are the good agreement of the EFG_3 parameters, $|Vzz|_3$ and $\eta_3 \sim 0$, obtained by annealing under XeF_2, with the simulation for δF =0.50, with interstitial fluorine rows along [100] and [010]. The simulated η~0 in this configuration is essentially due to the fact that, being the EFG the derivative of the electric field, Vxx becomes almost equal to Vyy along the EFG principal axis system. This is quite different on the other δF =0.50 configuration, where two interstitial F atoms are aligned along [110] axis that produces a big η ~ 042, never experimentally observed. On samples where after annealing under XeF_2, a last annealing step was done under Ar, the EFG_4 parameters fit quite well with the situation of a diluted concentration of fluorine, where Hg mainly sees one F at the center of the Hg mesh.

From the results and simulations we are led to the interpretation that only interstitial F at the center of the Hg square is found. For high concentrations the interstitial F prefer to order along [100], [010] directions. In this case, from the PAC fraction $f_3 \sim 68\ldots80\%$, due to the Hg (2x) coordination with F, we hint a fluorine concentration in the probing zone of δF ~ 0.34…0.40, that is above optimal F doping. By reducing the F concentration Hg then "sees" individual F atoms. From the PAC fraction f4 ~ 70…87%, due to the Hg (4x) coordination with F we hint now δF ~ 0.17…0.22 that is below/near optimum F doping [§].

[§] *A detailed publication of the described PAC data, EFG simulations and conclusions is being prepared.*

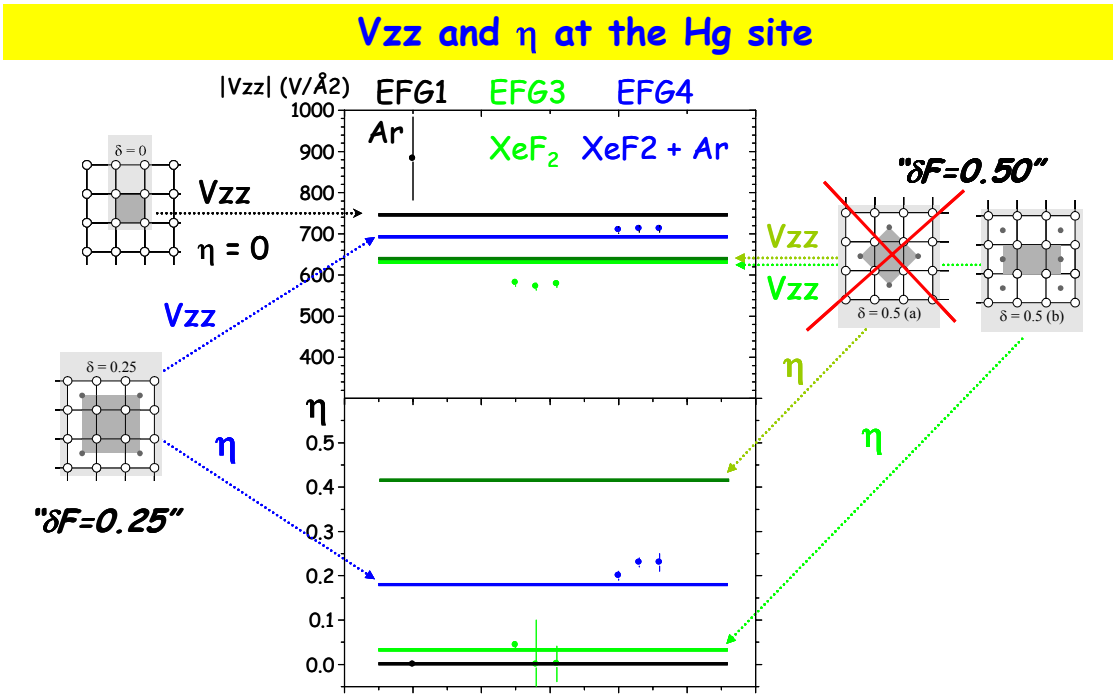

Figure 7 Experimental |Vzz| and η parameters of the EFGs obtained under different Ar and XeF_2 annealing conditions. For each experimental EFG the corresponding |Vzz| dot is plotted on the top graph while the corresponding η dot is plotted, along its vertical, on the graph below. The simulated |Vzz| and η parameters are plotted as horizontal lines which are assigned by arrows to the corresponding FLAPW simulations for the different F configurations.

3 Proposed work

Since Hg1201 cannot be doped with oxygen above $\delta_O \sim 23\%$, the collaboration is preparing to perform PAC studies on Hg1212 (n=2) and Hg1223 (n=3) where Tc is highest and the non-stoichiometric oxygen is easy to enter, with $\delta O >> 0.2$.

Phase 0 - Samples production and characterization at home laboratories.

Phase 1

a) PAC experiments are performed after annealing, or during annealing, under Ar, under Oxygen flow and under pressurized oxygen, with the aim of varying the sample's δO.
b) Fluorine doping, via soft-chemistry of XeF_2, will be tried for comparison.
c) The samples are returned to their home laboratories to be characterized.

Phase 2

a) If needed, phase 1a) shall be completed with missing data for systematic.
b) Low temperature PAC measurements shall be done, for few points below and above Tc. The aim is to observe any ordering change of the dopant in the normal state near Tc and in the superconducting state.
c) PAC measurements shall be done on Hg1223 epitaxial thin films. Single crystals of these materials are extremely rare and of too much reduced dimensions. The aim is to determine the orientation of the EFG principal system of axis, Vxx, Vyy and Vzz, with respect to the crystal lattice, improving the comparison of the experimental data with the EFG simulations for different oxygen configurations.

EFG simulations of oxygen doping, with relaxation allowed, are in course for several oxygen configurations starting from different initial un-deformed supercells, as was already mentioned in chapter 2.2. The two different configurations with $\delta O = 0.5$ are relatively easy to compute due to their smaller cells. Two additional configurations with $\delta O = 0.25$ and $\delta O = 0.125$, are being further implemented. These *diluted* oxygen models are particularly lengthy and time consuming but can provide essential data for typical low oxygen concentrations.

These experiments will confirm / not confirm the existence of a local chemical ordering of the dopant –oxygen- when present under high concentrations. The PAC measurements shall be compared with Tc and X-ray measurements, performed on the same samples at the home laboratories where the samples are produced. The local character of the proposed experiments is specific from the neighborhood of the Hg planes - which act as charge reservoirs - and can provide complementary information for the charge order mechanism in the high-Tc materials.

4 Experimental

4.1 Sample production and characterization

The samples of Hg1212 (n=2) and Hg1223 (n=3) are produced in powder form using the closed sealed ampoule vapor deposition technique in gradient furnaces [11, 18]. Epitaxial thin films of Hg1223 are produced with the ultrasonic spray pyrolysis technique [19].

To monitor the sample's crystalline structure and composition – at Grenoble – are used X-ray diffraction, Scanning Electron Microscopy (SEM), Transmission Electron Microscopy (TEM) and High Resolution TEM. To probe the thin films surface quality, orientation and to detect residual damage from implantation and annealing it will be used - at ITN – Rutherford Backscattering/Channeling (RBS/C). At the home-institutes χac susceptibility will be measured on powder samples and thin films. A SQUID is further available at –Porto- University. Resistivity is only measured in thin films, with the four-probe contact technique.

4.2 Equipment and Laboratories at ISOLDE

Storing and handling of samples is made inside dry glove boxes filled with N_2 to $P[O_2] < 3\%$. Each powder sample is implanted with ^{199m}Hg ($T_{1/2}$=42min) at 60keV to a low dose of 3 to 5.10^{12} at/cm^2 at RT, under vacuum of 5×10^{-6}mbar. On some thin films ^{197m}Hg ($T_{1/2}$ = 24h) will be implanted to a dose of 2.10^{13} at/cm^2. The implantations are done preferentially in the "old" solid-state-chamber, with beam sweeping and venting with N_2.

All PAC measurements are done in the ISOLDE off-line laboratory, building 275/R-011, http://cern.ch/isolde-offline , where the 6-detector γ–γ PAC (^{199m}Hg) and the e^--γ PAC spectrometer (^{197m}Hg) are working. Transport of sample holders and samples between the implantation chamber in the ISOLDE hall and the PAC laboratory is done under rough, dry vacuum (~0.1bar of N_2) on sealed boxes.

Several furnace systems exist which allow annealing under vacuum or under 1bar gas flow. Maximum annealing temperature will not exceed 200^{o}C. Pressurized annealings up to 20 bar are done with the samples kept inside specially cleaned and tidily sealed small Cu tubes. When annealing under (Ar, N2, O2) gas flow the furnaces are equipped with activated charcoal filters that trap volatile elements.

4.3 Beam time request

Samples to be probed with ^{199m}Hg require collection times of the order of 5 to 10 minutes per sample, every 4 to 5 hours. About 20 to 25 samples can be measured during a 5 days run. Samples to be measured with ^{197m}Hg require 30 to 60 minutes implantation time per sample. About 4 to 5 samples can be measured during a 5 to 7 days run.

As usual, optimization of such runs require sharing the same beam time with other users of the same target - molten Led with hot plasma ion source-.

We request 12 shifts divided in two groups, according Phase 1 and Phase 2 of experiments. The first beam time shall be scheduled from September 2004 and the second one, from May 2005. The time before the first run is essential for samples production and characterization. The time between the runs is needed for data analysis, samples characterization and optimization of the second set of experiments.

4.4 Deliverables

Paper publications and conference attendance for 2004 are being prepared in what regards the shortly described results on the fluorine doping. In what concerns people formation and thesis this research subject is addressed by three master and two PhD students. They integrate beam times, sharing afterwards the sample preparation and crystallographic/transport properties characterization and the analysis of the PAC results.

5 Further notes

-About point 2.3 from Add.1 “The doping of the Infinite Layer Cuprates”

Experiments on thin films of ILCs (MBE grown) could not perform due to lack of samples with enough thickness and good quality. We have then pursued research on samples from the BiSrCaCuO-ILCs nano-structures. It was reported that these materials show room temperature resistivity below 10^{-9} Ω.cm and have non-linear I (V) current / voltage relationship that suggest a superconductor behavior [20]. Since susceptibility measurements have not been able to show relevant diamagnetic properties because of the interference of the substrate signal, we performed PAC experiments using different probe nuclei, with the aim of disentangle if there were present magnetic fields. Unfortunately, on such highly non-stoichiometric materials there was no way of obtaining clear signals from the quadrupole contribution needed to observe any existing magnetic field below 1.5 T.

-During 2003 a web site has been implemented, still on a developing phase that accounts for activities of the solid state groups in the ISOLDE off-line laboratory 275, R-011. Previous papers from IS360, the proposal and Add.1 can be found in http://sslp.web.cern.ch/sslp/publications.php, under IS360.

References

1 Review on phenomenology, models, new ideas: Piers Coleman, Nature 424 (2003) 625; F.C. Zhang, Physics Review Letters 90 (2003) 207002-1.; J. Orenstein and A. J. Millis, Science 288 (2000) 468.

2 Review on Systematic of high-Tc families: M. Lagues, C.F. Beuran, C. Hatterer, P. Laffez, V. Mairet, C. Partiot, X. M. Xie, X.Z.Xu, C. Devill Cavellin, B. Eustache and C. Coussot, in: "Coherence in High Temperature Superconductors", eds. Guy Deutscher and Alex Revcolevschi (World Scientific, Singapore, 1996), p70

3 A synthesis review of the Hg-compounds, with references can be found on: IS360 Collaboration "Studies of High-Tc Superconductors Doped with Radioactive Isotopes", proposal - CERN/ISC 96-30, ISC P86 and Add.1-CERN / INTC 2000 – 039, INTC / P86 Add. 1. See http://sslp.web.cern.ch/sslp/publications.php, under IS360.

4 An interesting summary of technological issues can be found in http://www.eere.energy.gov/superconductivity/pdfs/2003_post_review_meeting.pdf.

5 A review on some application technologies: Shoji Tanaka, Future of IT, PT and superconductivity technology, Physica C 392–396 (2003) 1.

6 C.W. Chu, L. Gao, F. Chen, Z.J. Huang, R.L. Meng, Y.Y. Xue, Nature 365 1993 323; M. Nunez-Regueiro, J.L. Tholence, E.V. Antipov, J.J. Capponi, M. Marezio, Science 262 1993 97.

7 M.H. Julien, P. Carretta, M. Horvatic, C. Berthier, Y. Berthier, P. Ségransan, A. Carrington, and D. Colson, Phys. Rev. Lett. 76, 4238 (1996); M.H. Julien, M. Horvatic, P. Carretta, C. Berthier, Y. Berthier, P. Ségransan, S.M. Loureiro, and J.J. Capponi, Physica C268, 197 (1996); C.H. Booth, F. Bridges, E.D. Bauer, G.G. Li, J.B. Boyce, T. Claeson, C.W. Chu, and Q. Xiong, Phys. Rev. B52, R15745 (1995).

8 A. M. Abakumov, V. L. Aksenov, V. A. Alyoshin, E. V. Antipov, A. M. Balagurov, D. A. Mikhailova, S. N. Putilin and M. G. Rozova, Phys. Rev. Lett. 80 (1998) 385; S.N. Putilin, E.V. Antipov, A.M. Abakumov, M.G. Rozova, K.A. Lokshin, D.A. Pavlov, A.M. Balagurov, D.V. Sheptyakov, M. Marezio, Physica C 338 (2000) 52

9 J.T. Market, Y. Dalichaouch and M.B. Maple, in Physical Properties of High Temperature Superconductors I, ed. by D.M. Ginsberg (World Scientific, Singapore, 1989) p. 265; C.L. Chien, G. Xiao, M. Z. Cieplak, D. Musser, J.J. Rhyne and J.A. Gotaas, in Superconductivity and Its Applications, ed. H.S. Kwok and D.T. Shaw (Elsevier, New York, 1988) 110

10 S.M. Loureiro, E.V. Antipov, E.T. Alexandre, P.G. Radaelli, J.L. Tholence, J.J. Capponi and M. Marezio, in Proc. of Materials Aspects of High-Tc Superconductivity: 10 Years After the Discovery, NATO ASI Series E, Kluwer Acad. Publishes (1996).

11 A. Lanzara, N.L. Saini, A. Bianconi, F. Duc, and P. Bordet Phys. Rev. B59 (1999) 3851

12 P.Bordet, F. Duc, P.G. Radaelli, A. Lanzara, N. Saini, A. Bianconi and E.V. Antipov, Physica C 282-287 (1997) 1081

13 X. G. Zheng, C.N. Xu, Y. Tomokiyo, E. Tanaka, H. Yamada and Y. Soejima, Physics Review Letters 85 (2000) 5171

14 H. A. Mook, Pengcheng Dai and F. Dogan, Physics Review Letters 88 (2002) 097004-1

15 For a recent review see, e.g., S. A. Kivelson, I. P. Bindloss, E. Fradkin, V. Oganesyan, J. M. Tranquada, A. Kapitulnik and C. Howald, Reviews of Modern Physics 75 (2003) 1201; see also http://focus.aps.org/story/v9/st12.

16 J. G. Correia, J.P. Araújo, S.M. Loureiro, P. Toulemonde, S. Le Floch, P. Bordet, J. J. Capponi, R. Gatt, W.Tröger, B. Ctortecka, T. Butz, H.Haas, J. G. Marques, J.C. Soares, Physical Review B 61 (2000) 11769

17 J.P. Araújo, J.G. Correia, S.M. Loureiro, P. Toulemonde, S. Le Floch, P. Bordet, J. J. Capponi, W.Tröger, B. Ctortecka, H.Haas, R. Gatt, J.G. Marques, J.C.Soares, Physica C 341-348 (2000) 1969

18 V. A. Alyoshin, D. A. Mikhailova, and E. V. Antipov, Physica C271 (1996) 197

19 S. Phok, Ph. Galez, J.L. Jorda, Z. Supardi, D. De Barros, P. Odier, A. Sin, F. Weiss, Physica C372–376 (2002) 876

20 J.B. Moussy, J.Y. Laval, X.Z. Xu, F.C. Beuran, C. Deville Cavellin, M. Lagues, Physica C 329 (2000) 231; M. Lagues-M, X. Xiao-Ming, H. Tebbji, X. Xiang-Zhen, V. Mairet, C. Hatterer, C.F. Beuran, C. Deville-Cavellin, Science 262 (1993) 1850.